Efficient Solution Methods for Inverse Problems with Application to Tomography
Practical Tomography

Alfred K. Louis

Institut für Angewandte Mathematik
Universität des Saarlandes
66041 Saarbrücken
http://www.num.uni-sb.de
louis@num.uni-sb.de
and
http://www.isca-louis.com
louis@isca-louis.com

Novosibirsk NSU, October, 2011

UNIVERSITÄT DES SAARLANDES

Content

Content

Transmission Tomography

- X-Ray CT (Nobel Prize 1979)
- Phase Contrast Tomography
- Magnetic Resonance Imaging (Nuclear Magnetic Resonance; Nobel Prize 2003)
- Ultrasound CT
- Electromagnetic Waves
- Impedance
- Light
- Electron Paramagnetic Resonance Imaging
- Transmission Electron Microscopy

Emission Tomography

- PET
- SPECT
- EEG / MEG
- Bioluminescence Imaging

Nondestructive Testing

- Nondestructive Testing
  - X-Ray CT
  - Ultrasound
  - Microwaves
  - Backscattering X-Ray CT
  - Synchrotron Rays
  - Phase Contrast Tomography
  - Transmission Electron Microscopy

Historical Image

Leonardo da Vinci, 1500

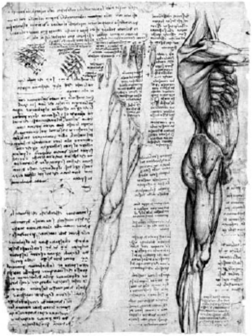

Leonardo da Vinci. Anatomische
Zeichnung. Um 1500

Historical Image

Hand of Dean of Röntgen, A.v. Koelliker, 23.01.1896

X-Ray CT

Content

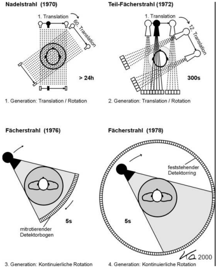
Nadelstrahl (1970)
1. Translation
60. Translation
> 24h
1. Generation: Translation / Rotation
Teil-Fächerstrahl (1972)
1. Translation
12. Translation
300s
2. Generation: Translation / Rotation
Fächerstrahl (1976)
5s
mitrotierender Detektorbogen
3. Generation: Kontinuierliche Rotation
Fächerstrahl (1978)
feststehender Detektorring
5s
2000
4. Generation: Kontinuierliche Rotation

Fan Beam Geometry

$$\mathbf{D}f(a,\theta) = \int_0^\infty f(a + t\theta)dt$$

Relation to Radon transorm

$$\mathbf{D}f = U\mathbf{R}f$$

where U is a unitary transform.

Transformation of the parallel geometry inversion to fan beam inversion.

Content

Basics

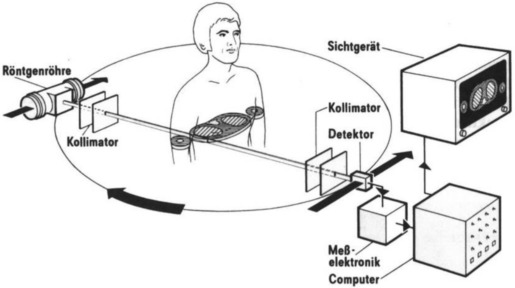
Röntgenröhre
Kollimator
Sichtgerät
Kollimator
Detektor
Meß-
elektronik
Computer

Typical Scanning Geometry in NDT

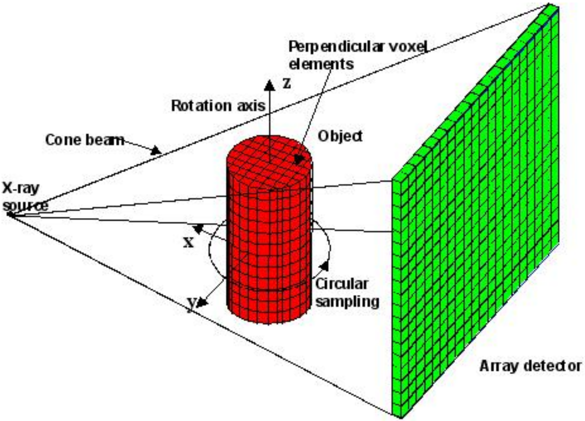

Some 3D Transforms

- 3D Radon Transform: $\mathbf{R}f(\theta, s) = \int_{\theta^\perp} f(s\theta + y)dy$

Some 3D Transforms

- 3D Radon Transform: $\mathbf{R}f(\theta, s) = \int_{\theta^\perp} f(s\theta + y)dy$
  Inversion Formula

$$f(x) = -\frac{1}{8\pi^2} \int_{S^2} (\mathbf{R}f)''(\theta, x^\top \theta) d\theta$$

Some 3D Transforms

- 3D Radon Transform: $\mathbf{R}f(\theta, s) = \int_{\theta^\perp} f(s\theta + y)dy$
  Inversion Formula

$$f(x) = -\frac{1}{8\pi^2} \int_{S^2} (\mathbf{R}f)''(\theta, x^\top \theta)d\theta$$

- 3D Parallel X - Ray Transform $\mathbf{P}f(\theta, y) = \int_{-\infty}^{\infty} f(y + t\theta)dt$

Some 3D Transforms

- 3D Radon Transform: $\mathbf{R}f(\theta, s) = \int_{\theta^\perp} f(s\theta + y)dy$
  Inversion Formula

$$f(x) = -\frac{1}{8\pi^2}\int_{S^2}(\mathbf{R}f)''(\theta, x^\top\theta)d\theta$$

- 3D Parallel X - Ray Transform $\mathbf{P}f(\theta, y) = \int_{-\infty}^{\infty} f(y + t\theta)dt$
  Inversion Formula

$$f = c\mathbf{P}^*\mathbf{I}^{-1}\mathbf{P}f$$

  where

$$\mathbf{I}^{-1}g(\xi) = |\xi|\hat{g}(\xi)$$

  and

$$\mathbf{P}^*g(x) = \int_{S^2} g(\theta, E_\theta x)d\theta$$

Some 3D Transforms

- 3D Radon Transform: $\mathbf{R}f(\theta, s) = \int_{\theta^\perp} f(s\theta + y)dy$
  Inversion Formula

$$f(x) = -\frac{1}{8\pi^2} \int_{S^2} (\mathbf{R}f)''(\theta, x^\top \theta) d\theta$$

- 3D Parallel X - Ray Transform $\mathbf{P}f(\theta, y) = \int_{-\infty}^{\infty} f(y + t\theta)dt$
  Inversion Formula

$$f = c\mathbf{P}^* \mathbf{I}^{-1} \mathbf{P}f$$

where

$$\mathbf{I}^{-1} g(\xi) = |\xi| \hat{g}(\xi)$$

and

$$\mathbf{P}^* g(x) = \int_{S^2} g(\theta, E_\theta x) d\theta$$

Too many data!

Synchrotron Measurements

Parallel X - Ray Transform for $\theta \in S^1 \times \{0\}$.
Then Transform

$$\mathbf{P} = \mathbf{P}_2 \otimes \mathbf{I}$$

Adapt 2D-Inversion (B. Hahn)

3D Synchrotron Data

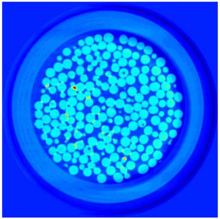

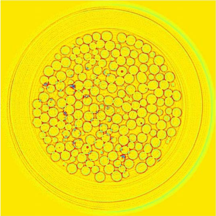

Better results using 3D algorthms: Bernadette HAHN

Big Challenge

Application: Determination of fluid flow in porous media

Big Challenge

Application: Determination of fluid flow in porous media
Object time dependent

Big Challenge

Application: Determination of fluid flow in porous media

Object time dependent

Data inconsistent for classical transform

3D Cone Beam : Mathematical Model

Source position: $a \in \Gamma$
Direction: $\theta \in S^2$

3D Cone Beam : Mathematical Model

Source position: $a \in \Gamma$
Direction: $\theta \in S^2$

$$\mathbf{D}f(a,\theta) = \int_0^\infty f(a + t\theta)dt$$

3D Cone Beam : Mathematical Model

Source position: $a \in \Gamma$
Direction: $\theta \in S^2$

$$\mathbf{D}f(a,\theta) = \int_0^\infty f(a+t\theta)dt$$

For flat detectors use other geometry

3D Cone Beam : Mathematical Model

Source position: $a \in \Gamma$
Direction: $\theta \in S^2$

$$\mathbf{D}f(a,\theta) = \int_0^\infty f(a+t\theta)dt$$

For flat detectors use other geometry
Compare with Radon transform in $\mathbb{R}^3$

$$\mathbf{R}f(\omega,s) = \int f(x)\delta(s - x^\top\omega)dx$$

Dual Transform

$$\mathbf{D} : L_2(\mathbb{R}^3) \to L_2(\Gamma \times S^2)$$

$$\mathbf{D}^* g(x) = \int_\Gamma |x - a|^{-2} g\Big(a, \frac{x - a}{|x - a|}\Big) da$$

Relation between Radon and Cone Beam Transform

Grangeat:

$$\frac{\partial}{\partial s}\mathbf{R}f(\omega, a^\top\omega) = -\int \mathbf{D}f(a,\theta)\delta'(\omega^\top\theta)d\theta$$

Proof:

$$\int \mathbf{R}f(\omega, s)\psi(s)ds = \int f(x)\psi(x^\top\omega)dx$$

$$\int \mathbf{D}f(a,\theta)h(\theta)d\theta = \int f(x)h\Big(\frac{x-a}{|x-a|}\Big)|x-a|^{-2}dx$$

Put $\psi(s) = \delta'(s - a^\top\omega)$ and $h(\theta) = \delta'(\theta^\top\omega)$ and use δ' homog. of degree -2 in $\mathbb{R}^3$.

References

- Hamaker, Smith, Solmon, Wagner, 1980
- Tuy, 1984
- Grangeat 1986
- Dietz 1999
- AKL, 2000
- Katsevich, 2000
- Zhao, Jiang, Zhuang, Wang, 2006
- ...

Inversion Formula

Theorem (AKL 2004)

Let the condition of Tuy-Kirillov be fulfilled. Then the Inversion formula can be given as

Inversion Formula

Theorem (AKL 2004)

Let the condition of Tuy-Kirillov be fulfilled. Then the Inversion formula can be given as

$$f = -\frac{1}{8\pi^2} D^* T M_{\Gamma,a} T D f$$

where

$$D^* g(x) = \int_\Gamma |x-a|^{-2} g(a, \frac{x-a}{|x-a|}) da$$

$$Tg(\omega) = \int_{S^2} g(\theta)\delta'(\theta^\top \omega) d\theta$$

$$M_{\Gamma,a} h(\omega) = |a'^\top \omega| m(\omega, a^\top \omega) h(\omega)$$

Crofton Symbol

$$m = 1/n$$

where n is the Crofton symbol, counting how often a plane trhough a point cuts the source path Γ
Hence $n \in \mathbb{N}_0$ and therefore
m is not differentiable!

Challenge

Inversion formula contains detailed information about curve Γ.
But in practice measurements are taken only at discrete points.
How to include in algorithms?

Images

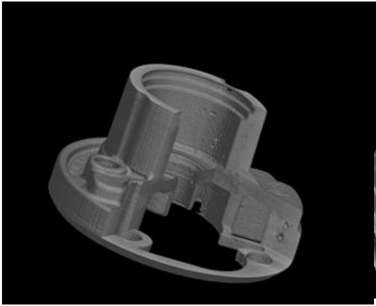

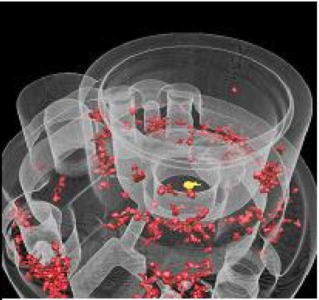

Images

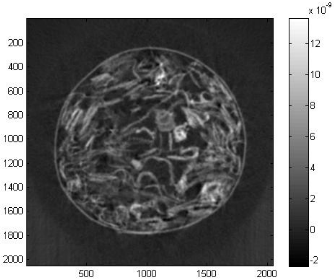
x 10^-9
200
400
600
800
1000
1200
1400
1600
1800
2000
500
1000
1500
2000
12
10
8
6
4
2
0
-2

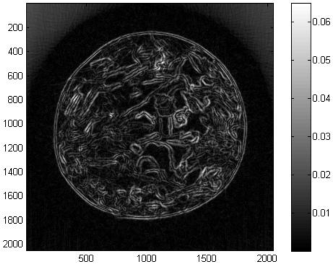
200
400
600
800
1000
1200
1400
1600
1800
2000
500
1000
1500
2000
0.06
0.05
0.04
0.03
0.02
0.01

Reconstruction Kernel

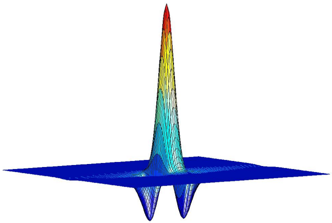

Data from DKFZ

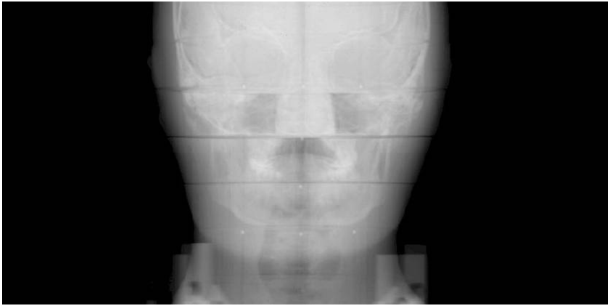

Reconstruction

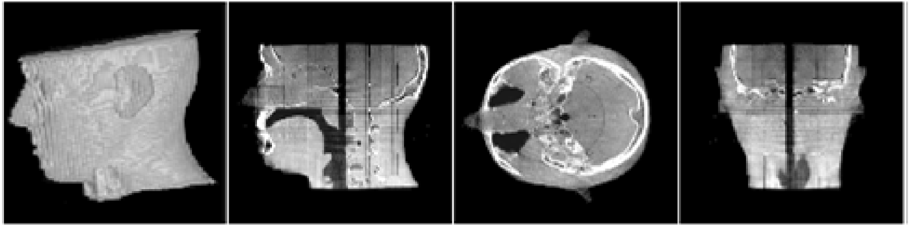

Surprise Egg

Data from IzfP

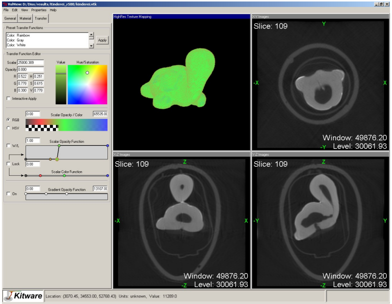

Comparison with Method of Katsevich

Comparison with Method of Katsevich

- Katsevich uses π - lines

Comparison with Method of Katsevich

- Katsevich uses π - lines
- hence integration over parts of Γ where n is constant

Comparison with Method of Katsevich

- Katsevich uses π - lines
- hence integration over parts of Γ where n is constant
- Backprojection depends on reconstruction point x

Comparison with Method of Katsevich

- Katsevich uses π - lines
- hence integration over parts of Γ where n is constant
- Backprojection depends on reconstruction point x
- Jump of n at the end introduces δ - distributions, hence point evaluation of data

Laminography

Application for example: printed circuit board

- Data given in very small range

Laminography

Application for example: printed circuit board

- Data given in very small range
- Classical Algorithms fail

Laminography

Application for example: printed circuit board

- Data given in very small range
- Classical Algorithms fail
- So far: Iterative algorithms realized on graphical processors (GPU)

Laminography

Application for example: printed circuit board

- Data given in very small range
- Classical Algorithms fail
- So far: Iterative algorithms realized on graphical processors (GPU)
- Optimizing order of used equations

Laminography

Application for example: printed circuit board

- Data given in very small range
- Classical Algorithms fail
- So far: Iterative algorithms realized on graphical processors (GPU)
- Optimizing order of used equations
- Use a priori information (see Lavrentiev)

Importance of Mathematics